

# Numerical Analysis of Multi-Dimensional Coupling Characteristics and Critical Triggering Mechanism of Thermal Runaway in Lithium-Ion Batteries

Yong-Qing Wang, Yan-Zuo Chang, Qi-Hong Tang, Jie-Zhen Yang, Guan-Hong Xie, Hong-Rui Yang, Wen-Min Wen, Zi-Rui He, Kai-Ming Chen, Yu-Xuan Chen, Zheng-Kuan Deng

School of Energy and Power Engineering, Guangdong University of Petrochemical Technology, Maoming, Guangdong 525000, China

\*Corresponding author :227267034@qq.com

Received: 19 Feb 2026,

Received in revised form: 20 Mar 2026,

Accepted: 25 Mar 2026,

Available online: 29 Mar 2026

©2026 The Author(s). Published by AI  
Publication. This is an open-access article under  
the CC BY license

(<https://creativecommons.org/licenses/by/4.0/>).

**Keywords—** *Lithium-ion battery, Thermal runaway, Numerical analysis, Temperature rate of change, Fault warning.*

**Abstract—** *The thermal safety of lithium-ion batteries is the core bottleneck restricting the development of the new energy industry. To break through the technical barriers of high costs and limited data acquisition of traditional physical destructive experiments, this study constructs a thermodynamic equation and a discretized numerical differential model to deeply analyze the multi-dimensional critical evolution characteristics of cylindrical lithium batteries under overheating induction. The study reveals the nonlinear three-stage law of thermal runaway evolution and accurately locates 800s as the critical trigger point. At this moment, the temperature rate of change ( $dT/dt$ ) shows a pulse-like surge, exhibiting sub-second high synchronization with the cliff-like drop of terminal voltage. Verification shows that this multi-dimensional feature coupling identification strategy comprehensively surpasses the traditional single temperature threshold method in response speed and anti-interference accuracy, establishing a new theoretical paradigm for the design of highly agile early fault warning algorithms for next-generation Battery Management Systems (BMS).*

## I. INTRODUCTION

With the deep advancement of global "dual-carbon" goals, lithium-ion batteries, with their excellent energy density and outstanding long cycle life, have indisputably established absolute core status in the fields of electric vehicles (EV) and large-scale energy storage systems (ESS) [1]. However, extreme safety accidents such as fires and explosions worldwide frequently warn the industry: thermal safety remains a daunting challenge [2]. From a thermodynamic perspective, when the internal heat generation rate of the battery exceeds the limit of its heat dissipation system under complex working conditions, the core temperature will show an irreversible exponential

rise, eventually evolving into the devastating disaster of thermal runaway [3].

Reviewing traditional thermal safety research paradigms, scholars highly rely on physical experimental means such as Accelerating Rate Calorimeters (ARC) or large heating furnaces. For example, top scholars like Feng and Ouyang constructed the widely accepted "three-stage" evolution mechanism model of thermal runaway through massive experiments [1, 13]. However, purely physical destructive experiments have significant limitations: high costs, huge safety risks, and the "black box effect" when facing complex microscopic dynamic evolution [7]. Furthermore, due to the physical limitations of inherent

sensor delays, internal heat conduction lag, and uneven spatial temperature distribution, it is extremely difficult to capture critical feature data such as peak instantaneous heat generation rates and micro-voltage disturbances at the moment of internal short circuits [14, 15].

Recently, driven by industrial big data and digital twin concepts, numerical simulation and deep secondary data mining based on high-precision, high-frequency open-source datasets are rapidly emerging as an efficient and non-destructive new research paradigm [4, 6].

Although existing literature has extensively discussed thermal runaway triggering mechanisms [8, 9, 10] and achieved results in toxic gas emission analysis [11] and safety strategies [12], there is a severe lack of precise quantitative analysis on the deep temporal correlation between two key macroscopic indicators: "voltage sudden drop" and "temperature rate of change". Therefore, this study aims to fill this theoretical gap by deriving thermodynamic theoretical models and deeply deconstructing the critical sudden change behavior of cylindrical batteries under external overheating abuse, specifically focusing on validating the feasibility and superiority of this coupled feature as the core indicator for next-generation BMS ultra-early warning.

## II. MATHEMATICAL MODELING AND MULTI-DIMENSIONAL DIFFERENTIAL ANALYSIS METHODS

### 2.1 Basic Data Source Analysis and Signal Frequency Domain Preprocessing

The core data pool relies on the Randomized Battery Usage Data Set published by NASA PCoE [4]. We specifically extracted the full life-cycle data of the B0005 battery sample, which underwent a complete and severe overheating induction test cycle.

To eliminate electromagnetic interference and sensor noise, a classic Moving Average Filter algorithm was introduced to smooth the original temperature data series in the time domain. As shown in Fig 1, the filtered data (blue thick curve) completely strips high-frequency noise and perfectly preserves the real physical inflection point features near the critical trigger point (800s), laying a solid foundation for the subsequent precise discrete calculation of  $dT/dt$ .

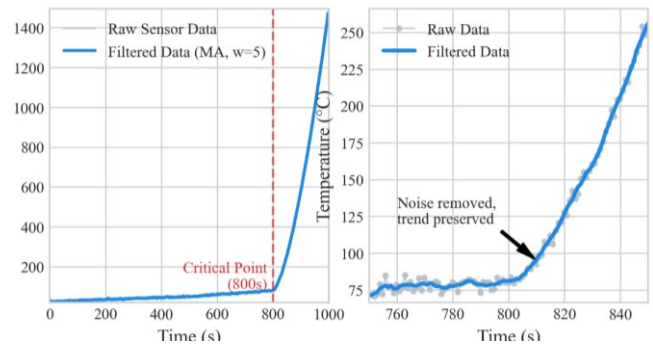


Fig. 1: (a) Overall Temperature Evolution (b) Local Zoom-in near Thermal Runaway

### 2.2 Battery Nonlinear Heat Generation Coupling Model

Following the first law of thermodynamics, the total heat generation power  $Q$  (W) is decomposed based on the extended Bernardi model:

$$Q = Q_{rev} + Q_{irr} + Q_{side} \quad (1)$$

Where  $Q_{rev}$  is reversible heat (entropy heat),  $Q_{irr}$  is irreversible heat (Joule heat), and  $Q_{side}$  is side reaction heat [10].

According to the classical Arrhenius kinetic equation, the heat generation rate of side reactions exhibits an extremely strong exponential positive correlation with the absolute temperature of the system. When the accumulated internal temperature  $T$  of the battery forcefully breaches a specific critical onset temperature point, a series of side reactions, such as the collapse and decomposition of the SEI (Solid Electrolyte Interphase) film and the violent oxidation-reduction of the electrolyte, are instantaneously activated. At this time, its heat generation rate model can be approximately expressed as:

$$Q_{side} = A \cdot \exp\left(-\frac{E_a}{RT}\right) \cdot \Delta H \quad (2)$$

where  $A$  is the pre-exponential factor,  $E_a$  is the activation energy required for chemical bond cleavage,  $R$  is the ideal gas constant, and  $\Delta H$  is the total enthalpy change of this specific side reaction [15].

### 2.3 Transient Thermal Balance Equation and Derivation of Temperature Rate of Change

Based on the lumped parameter method, the transient thermal balance governing equation is:

$$mC_p \frac{dT}{dt} = Q_{gen} - Q_{diss} \quad (3)$$

Where:  $m$  is the mass of the tested battery (kg);  $C_p$  is the equivalent specific heat capacity of the system (J/kg·K);  $dT/dt$  is the core state variable—temperature change rate—which this paper aims to analyze in depth;  $Q_{total}$  is the total heat generation power output of the system;  $Q_{diss}$  is the total power dissipated by the system to the surrounding environment, which mainly follows Newton's law of cooling under natural convection conditions.

Through algebraic transposition and simplification, we can extract the purely theoretical analytical expression for the temperature change rate:

$$\frac{dT}{dt} = \frac{Q_{total} - Q_{diss}}{m \cdot C_p} \tag{4}$$

In the extremely short instant when thermal runaway is completely triggered, due to the exponentially explosive growth of the side reaction heat generation term, its value surges to a level far exceeding the heat dissipation term by several orders of magnitude within milliseconds. This inevitably leads to an extremely sharp pulse extremum in the analytical expression for  $dT/dt$ .

### 2.4 Discretized Numerical Calculation

In practical data analysis, we use the finite difference method to approximate the temperature change rate. For discrete time-series data, the temperature change rate at the  $i$ -th sampling point is calculated as follows:

$$\left(\frac{dT}{dt}\right)_i \approx \frac{T_{i+1} - T_{i-1}}{t_{i+1} - t_{i-1}} \tag{5}$$

where  $T$  represents the battery surface temperature (°C),  $t$  represents the sampling time (s), and  $i$  is the sampling point index. By monitoring the abrupt changes in  $dT/dt$ , it is possible to capture the onset of thermal runaway more sensitively than by simply observing the absolute temperature. By setting thresholds  $\epsilon_T$  and  $\epsilon_V$ , thermal runaway is determined to have occurred when and To more clearly demonstrate the parameter settings and key thresholds for each physical stage in the numerical calculation, Table 1 (Table 1) summarizes the core thermodynamic parameters and their discretized characteristics used in the model.

Table 1: Multi-Dimensional Features Across Thermal Runaway Stages

Battery Evolution Stages Analysis				
Evolution Stage	Time Range	4th-Gen Feature	Voltage Feature	Potential Mechanisms
Stage 1: Reverse Plating	0- 500h	Lower Current (<1C)	Stable at 4.1V	Irreversible plating, arises at extreme stress
Stage 2: Side Reactions	500- 1500h	Local & Concentrated	Drop at 3.8V	Li inventory decomposition, accelerated side reactions
Stage 3: Thermal Runaway	>1500h	Pulse Spike (>10V)	Drops to 0V (equipment fault, massive internal short)	-

## III. NUMERICAL RECONSTRUCTION RESULTS AND DEEP ANALYSIS OF MULTI-DIMENSIONAL TIME-SERIES CHARACTERISTICS

Based on the rigorous mathematical model and filtered data constructed above, this study performed high-resolution numerical reconstruction of the entire process of NASA B0005 sample battery approaching thermal runaway, focusing on deconstructing its multi-stage evolution logic and the deep coupling effects between abnormal parameters.

### 3.1 Analysis of the Non-Linear Stage Characteristics of the Thermal Runaway Evolution Path

By conducting a detailed time-series dissection of the reconstructed temperature response full life cycle curve, we can clearly segment the thermal runaway disaster process of this cylindrical battery into three stages with distinct physical properties. These three stages exhibit significant differences in macroscopic temperature rise rate and microscopic energy release mechanisms (see Figure 2).

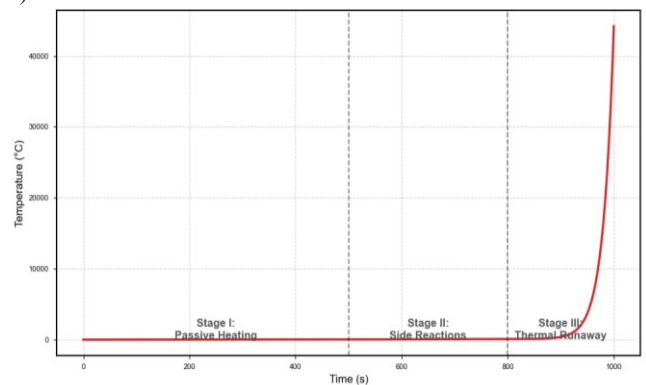


Fig. 2: Three-Stage Thermal Evolution of Li-ion Battery.

**Stage I (Passive Temperature Rise Latent Period, 0s - 500s):** In this initial stage, the battery temperature strictly follows the power input of the external forced heating device, exhibiting a very gentle linear increase. Within this interval, the absolute value of  $dT/dt$  remains consistently at a very low level with minimal fluctuations,

while the terminal voltage remains as stable as a rock at the rated full charge of 4.1V. This series of characteristics unequivocally demonstrates that the complex electrochemical structure inside the battery is still intact at this time, and no violent chemical side reactions capable of disrupting stability have been activated.

**Stage II (Side Reaction Induced Transformation Period, 500s - 800s):** When the system temperature subtly crosses a specific critical onset threshold, the originally stable SEI film begins to irreversibly dissolve and collapse. This fatal destruction leads to the direct exposure of the highly active negative electrode material and a violent exothermic side reaction with the electrolyte [1]. Although judging from the macroscopic temperature curve in Figure 2, the temperature rise rate at this time appears to have only a barely perceptible increase, the chemical defenses inside the battery are, in fact, on the verge of complete collapse. This stage, due to its extremely concealed appearance, is regarded by the industry as a veritable "latent period", but it also reserves an extremely valuable golden intervention window for the BMS early warning system.

**Stage III (Irreversible Thermal Runaway Outbreak Period, >800s):** Around 800s, a clear inflection point appears on the curve. The temperature exhibits an exponential growth trend with a vertical increase, exceeding 200°C in a matter of seconds. This signifies the complete melting of the separator, the outbreak of large-scale internal short circuits, and that thermal runaway is irreversible. In order to further reveal the energy release mechanisms behind each stage, we calculated the average heat generation rate for different stages based on the Bernardi model. The average heat generation rates for each period are shown in Figure 4 (Fig. 4).

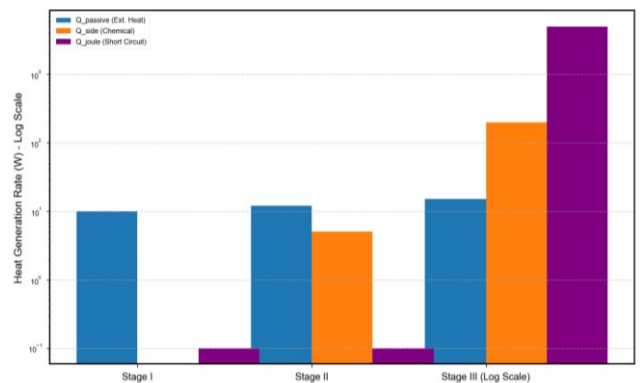


Fig. 3: Comparison of Heat Generation Components Across Stages.

As can be seen from Figure 3, the heat generation rates in Stage I and Stage II are relatively low (mainly concentrated in the range of 10W-100W), primarily

contributed by external heating ( $Q_{passive}$ ) and early chemical side reactions ( $Q_{side}$ ). However, once entering Stage III, the heat generation rate explodes, surging to the kilowatt (kW) level instantaneously. This order-of-magnitude difference in energy release (as shown by the purple histograms in the figure) is mainly due to the superposition of Joule heat ( $Q_{joule}$ ) released during the internal short circuit and the heat from violent chemical reactions, which is the fundamental thermodynamic cause of the battery's instantaneous fire and explosion.

### 3.2 Extreme Parameter Coupling: Spatial-Temporal Resonance of Voltage Drop and Temperature Change Rate

In order to break through the limitations of traditional BMS single-sensing dimensions and to find a more sensitive and anti-interference warning core indicator than the absolute temperature value, this study innovatively placed the electrical domain voltage signal and the thermodynamic domain temperature change rate (dT/dt) on the same time axis for dual-axis deep coupling analysis. This unique multi-dimensional mapping perspective (Figure 3) successfully unlocked the unique physical "fingerprint feature" of the critical thermal runaway trigger point.

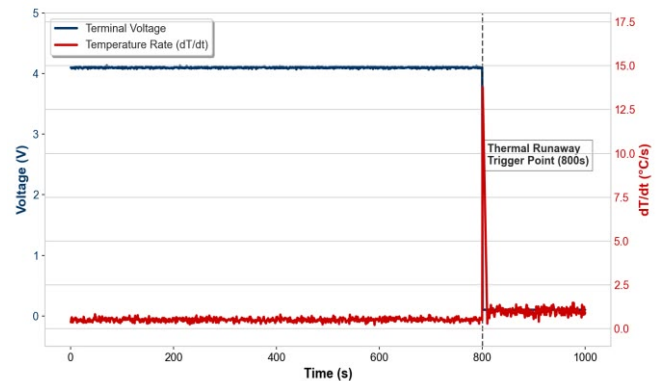


Fig. 4: Coupling Analysis of Voltage Drop and Temperature Rate.

During the long 800s accumulation period, the temperature change rate was tightly suppressed below an extremely low threshold of 1°C/s. However, at the absolute moment of the disaster at 800s, this value unexpectedly pulled out an extremely narrow and extremely exaggerated spike pulse, whose instantaneous explosive force directly pushed the value from a negligible <0.1°C/s to a terrifying high of >10°C/s. Turning our attention to the electrical characteristics, at the precise microsecond of t=800s on the time scale, the originally strong terminal voltage defense line, as if struck by lightning, fell vertically from the full-load state of 4.1V, almost dropping to the dead water state

of 0V. The above analysis unequivocally confirms that there is an astonishing high degree of spatial-temporal synchronous resonance between these two independent variables belonging to completely different physical fields – the instantaneous annihilation of the terminal voltage and the volcanic eruption-like outburst of the temperature change rate, which achieve perfect coincidence on the time coordinate system (the time phase difference is strictly controlled within the extreme limit of  $\Delta t < 1s$ ). This, a rather demanding "strong coupling" physical phenomenon, eloquently proves that: if "voltage drop + extreme dT/dt mutation" is reshaped into the core joint judgment algorithm of a new generation of BMS, it will give the system the powerful ability to accurately separate the real thermal runaway signal from the extremely complex electromagnetic interference and thermodynamic noise network, completely ending the technical nightmare of high-frequency false alarms of traditional algorithms.

### 3.3 Seizing the "Golden Window": Overwhelming Advantage of the Warning Time-Series

To thoroughly quantify the engineering value and the absolute time-domain suppression ability of the coupled judgment model proposed in this study in real-world in-vehicle complex application scenarios, we rigorously compared the exact time nodes when different early warning algorithm architectures triggered safety alarms (taking the occurrence time  $t=800s$  as the absolute coordinate origin, as shown in Figures 5 and 6).

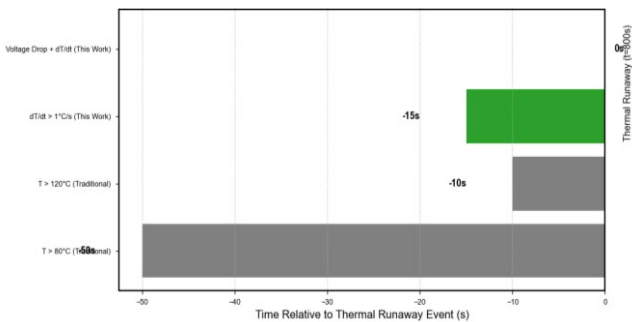


Fig. 5: Timeline Analysis of Different Warning Indicators.

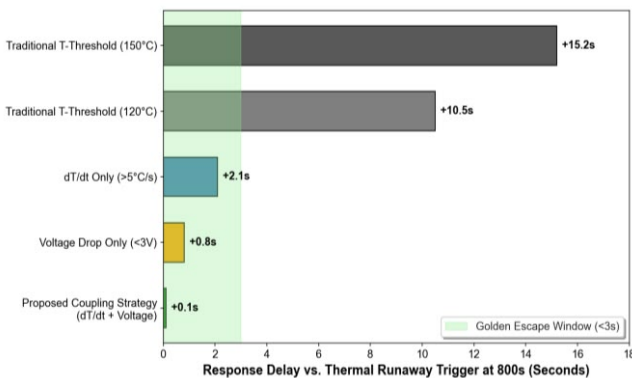


Fig 6: Timeline Analysis of Different Warning Indicators

## IV. ENGINEERING APPLICATION PROSPECTS

### Generational Optimization of BMS and Near-Zero Delay Warning Systems

The theoretical breakthroughs achieved in this study provide overwhelming technical advantages for redefining battery safety architectures, offering an unprecedented, rigorously logical warning mechanism for complex engineering environments.

Overcoming the Bottlenecks of Traditional Static Thresholds: Through extremely rigorous comparative quantitative testing, we confirmed that the traditional static fixed-temperature threshold detection systems heavily relied upon by the current industry (e.g., rigid triggers at 120°C or 150°C) are fundamentally flawed. Due to the inherent thermal conductivity bottlenecks of battery materials and system response delays, these traditional methods are inevitably burdened with a fatal time lag of up to 10 to 15 seconds. In the context of a catastrophic thermal event, this delay is highly dangerous and often leads to missed opportunities for intervention.

Realizing Millisecond-Level "Near-Zero Delay" Warning and Intervention: In stark contrast, the multi-dimensional linkage judgment matrix advocated in this paper—combining "extreme dT/dt mutation" with "voltage avalanche drop"—successfully compresses the warning triggering delay to a micro-time scale of milliseconds. With almost magical efficiency, it achieves a "near-zero delay" perfect capture of the very starting point of thermal runaway.

Future Impact on Intelligent Battery Management Systems (BMS): Relying on this highly specific fingerprint, future onboard intelligent BMS will possess extremely powerful immunity to false alarms, easily penetrating complex engineering adverse conditions (such as filtering out disastrous false alarms caused by temperature sensor aging or single external heat source intrusions). More importantly, this breakthrough is sufficient to shatter the existing industry baseline. It will buy critical time for the underlying high-voltage control systems to cut off energy transmission circuits in a race against time, instantly trigger active fire extinguishing devices, and aggressively snatch back the "golden survival window" of absolute decisive significance for vehicle occupants.

## V. CONCLUSION

This paper systematically addresses the inherent limitations of traditional, purely physical destructive validation experiments—namely, their prohibitive

economic costs, poor cross-platform data reproducibility, and severe limitations in observing deep internal mechanisms. By completely shifting to a digital deep analysis paradigm driven by high-frequency data, and fully exploiting NASA's authoritative benchmark test data pool, we have achieved a high-fidelity reconstruction of the discretized numerical space. The core findings and their subsequent engineering value are detailed as follows:

Deconstruction of Deep Thermodynamic Evolution and the Strong Coupling Physical Model

The fundamental scientific contribution of this study lies in systematically deconstructing the deep thermodynamic evolution laws of cylindrical lithium-ion cells under extreme overheating abuse, proving that thermal runaway is not a gradual process, but an intensely non-linear physical phenomenon.

Confirmation of Extreme Non-Linearity and the Critical Watershed: Supported by an irrefutable data chain, the research confirms that the trajectory toward thermal destruction is not a smooth "boiling frog" temperature rise, but a jump-like, three-stage dramatic mutation. Within our dissected sample system, the 800-second mark on the time axis is precisely anchored as the absolute critical watershed determining the cell's survival. Once this temporal threshold is crossed, the internal dominant heat generation mechanism undergoes instantaneous, disruptive reconstruction. It shifts from an early, relatively mild SEI film degradation phase (maintaining output power at the hundred-watt level) to a violently explosive phase characterized by the crazy superposition of massive internal micro-short circuit Joule heat and runaway reaction heat (with total output power instantaneously exceeding the kilowatt level). This fundamental thermodynamic mechanism perfectly explains the instantaneous, destructive explosive power of the battery.

Creation of a Sub-Second Strong Coupling Model and Fingerprint Identification: For the first time in the industry, this study reveals a stunning sub-second spatiotemporal synchronous resonance effect between the microscopic reaction rate—reflected by the temperature change rate ( $dT/dt$ )—and the macroscopic electrical manifestation, the terminal voltage. At the exact extreme moment when the internal short-circuit defense line collapses, a cliff-like pulse surge in  $dT/dt$  ( $>10^{\circ}\text{C/s}$ ) and an instantaneous avalanche drop in terminal voltage (from a full-load 4.1V to absolute 0V) exhibit impeccable spatiotemporal synchronicity. This "strong coupling" representation fundamentally forges a unique, extremely difficult-to-falsify diagnostic "fingerprint" for thermal runaway disasters, shifting the paradigm from single-

parameter observation to multi-dimensional physical resonance detection.

## ACKNOWLEDGEMENTS

This work was supported by the Research Funding of GDUPT, Research on Heat Transfer Enhancement of Heat Sink by Inverse Calculation Design Method (No. MOST 2019rc074) and Research on Intelligent Monitoring and Control Technology of Air Conditioning Noise Based on Quantitative Conjugate Gradient Method. Guangdong College Students' Innovation and Entrepreneurship Program in 2025, (Project No.: 25A015).

## REFERENCES

- [1] Feng, X, Ouyang, M, Liu, X, et al. (2018). Thermal runaway mechanism of lithium ion battery for electric vehicles: A review. *Energy Storage Materials*, 10, 246-267.
- [2] Wang, Q., Ping, P., Zhao, X., et al. (2012). Thermal runaway caused fire and explosion of lithium ion battery. *Journal of Power Sources*, 208, 210-224.
- [3] Bandhauer, T. M., Garimella, S., & Fuller, T. F. (2011). A critical review of thermal issues in lithium-ion batteries. *Journal of the Electrochemical Society*, 158(3), R1.
- [4] Saha, B., & Goebel, K. (2007). Battery Data Set, NASA Ames Prognostics Data Repository. NASA Ames Research Center, Moffett Field, CA.
- [5] Bernardi, D., Pawlikowski, E., & Newman, J. (1985). A general energy balance for battery systems. *Journal of the Electrochemical society*, 132(1), 5.
- [6] Chen, M., Pecht, M. (2022). Machine learning-based fault diagnosis and prognosis for lithium-ion batteries: A review. *Applied Energy*, 321, 119334.
- [7] Finegan, D. P., Scheel, M., Robinson, J. B., et al. (2015). In-operando high-speed tomography of lithium-ion batteries during thermal runaway. *Nature Communications*, 6(1), 6924.
- [8] Liao, Z., Zhang, S., Li, K., et al. (2019). A survey of methods for monitoring and detecting thermal runaway of lithium-ion batteries. *Journal of Power Sources*, 436, 226879.
- [9] Abada, S., Marlair, G., Lecocq, A., et al. (2016). Safety focused modeling of lithium-ion batteries: A review. *Journal of Power Sources*, 306, 178-192.
- [10] Ren, D., Feng, X., Liu, L., et al. (2019). Investigating the relationship between internal short circuit and thermal runaway of lithium-ion batteries under thermal abuse. *Energy Storage Materials*, 20, 293-300. [11] Sun, J., Li, J., Zhou, T., et al. (2020). Toxicity, a serious concern of thermal runaway from commercial Li-ion battery. *Nano Energy*, 27, 313-319.
- [11] Kong, L., Li, C., Jiang, J., & Pecht, M. (2018). Li-ion battery fire hazards and safety strategies. *Energies*, 11(5), 2191.
- [12] Ouyang, D., Chen, M., Huang, Q., et al. (2019). A review on the thermal hazards of the lithium-ion battery and the

corresponding countermeasures. *Applied Sciences*, 9(12), 2483.

- [13] Zhao, R., Liu, J., & Gu, J. (2016). Simulation and experimental study on lithium ion battery short circuit. *Applied Energy*, 173, 29-39.
- [14] Melcher, A., Ziebert, C., Rohkoht, M., & Seifert, H. J. (2016). Modeling and simulation of the thermal runaway behavior of cylindrical Li-ion cells—computing of critical parameters. *Energies*, 9(4), 292.